Available online at www.sciencedirect.com
SCIENCE DIRECT®
Physics of the Earth and Planetary Interiors 143–144 (2004) 145–156
PHYSICS OF THE EARTH AND PLANETARY INTERIORS
www.elsevier.com/locate/pepi

High-pressure transitions of diopside and wollastonite: phase equilibria and thermochemistry of $CaMgSi_2O_6$, $CaSiO_3$ and $CaSi_2O_5$–$CaTiSiO_5$ system

M. Akaogi*, M. Yano, Y. Tejima, M. Iijima, H. Kojitani

Department of Chemistry, Gakushuin University, 1-5-1 Mejiro, Toshima-ku, Tokyo 171-8588, Japan

Received 4 January 2003; received in revised form 23 June 2003; accepted 6 August 2003

Abstract

Phase transitions of $CaMgSi_2O_6$ diopside and $CaSiO_3$ wollastonite were examined at pressures to 23 GPa and temperatures to 2000 °C, using a Kawai-type multiavil apparatus. Enthalpies of high-pressure phases in $CaSiO_3$ and in the $CaSi_2O_5$–$CaTiSiO_5$ system were also measured by high-temperature calorimetry. At 17–18 GPa, diopside dissociates to $CaSiO_3$-rich perovskite + Mg-rich (Mg,Ca)SiO_3 tetragonal garnet (Gt) above about 1400 °C. The solubilities of $CaSiO_3$ in garnet and $MgSiO_3$ in perovskite increase with temperature. At 17–18 GPa below about 1400 °C, diopside dissociates to Ca-perovskite + β-Mg_2SiO_4 + stishovite. The Mg, Si-phases coexisting with Ca-perovskite change to γ-Mg_2SiO_4 + stishovite, to ilmenite, and finally to Mg-perovskite with increasing pressure. $CaSiO_3$ wollastonite transforms to the walstromite structure, and further dissociates to Ca_2SiO_4 larnite + $CaSi_2O_5$ titanite. The latter transition occurs at 9–11 GPa with a positive Clapeyron slope. At 1600 °C, larnite + titanite transform to $CaSiO_3$ perovskite at 14.6 ± 0.6 GPa, calibrated against the α–β transition pressure of Mg_2SiO_4. The enthalpies of formation of $CaSiO_3$ walstromite and $CaSi_2O_5$ titanite from the mixture of CaO and SiO_2 quartz at 298 K have been determined as −76.1 ± 2.8, and −27.8 ± 2.1 kJ/mol, respectively. The latter was estimated from enthalpy measurements of titanite solid solutions in the system $CaSi_2O_5$–$CaTiSiO_5$, because $CaSi_2O_5$ titanite transforms to a triclinic phase upon decompression. The enthalpy difference between titanite and the triclinic phase is only 1.5 ± 4.8 kJ/mol. Using these enthalpies of formation and those of larnite and $CaSiO_3$ perovskite, the transition boundaries in $CaSiO_3$ have been calculated. The calculated boundaries for the wollastonite–walstromite–larnite + titanite transitions are consistent with the experimental determinations within the errors. The calculated boundary between larnite + titanite and Ca-perovskite has a slope of 1.3–1.8(±0.4) MPa/K, and is located at a pressure about 2 GPa higher than that determined by [Am. Mineral. 79 (1994) 1219].

Keywords: Diopside; Wollastonite; Titanite; Ca-perovskite; High-pressure transition; Calorimetry

1. Introduction

$CaMgSi_2O_6$ diopside is a major component of clinopyroxene (Cpx) in the crust and upper mantle. $CaSiO_3$ wollastonite is an important ceramic and cement substance, and its high-pressure polymorph with the perovskite structure is accepted as one of major

* Corresponding author. Tel.: +81-3-3986-0221; fax: +81-3-5992-1029.
E-mail address: masaki.akaogi@gakushuin.ac.jp (M. Akaogi).

0031-9201/$ – see front matter © 2004 Elsevier B.V. All rights reserved.
doi:10.1016/j.pepi.2003.08.008

constituent minerals of the lower mantle. Although a number of studies on diopside have been performed at high-pressure, phase relations of diopside have not yet been fully clarified. For example, Canil (1994) reported that diopside first dissociates to $CaSiO_3$ perovskite + $MgSiO_3$ ilmenite at about 18 GPa below 1300 °C, while Oguri et al. (1997) revealed dissociation to $CaSiO_3$ perovskite + β-Mg_2SiO_4 + stishovite at almost the same conditions. Therefore, we have examined the detailed phase relations of diopside at high pressures and high temperatures in this study.

At around 1200 °C, $CaSiO_3$ wollastonite transforms to the walstromite structure at about 3 GPa, and further dissociates to Ca_2SiO_4 larnite + $CaSi_2O_5$ titanite at about 10 GPa. The two phases combine to form $CaSiO_3$ perovskite at about 12–16 GPa. The perovskite phase cannot be quenched but transforms to an amorphous phase on release of pressure. The wollastonite-walstromite transition was accurately determined using piston-cylinder apparatus (Essene, 1974; Huang and Wyllie, 1975). Among the two-phase assemblage, $CaSi_2O_5$ titanite, which has both four- and six-fold coordinated Si, converts at least in part to a triclinic phase having five-fold coordinated Si upon decompression (Kanzaki et al., 1991; Angel, 1997). Although the formation pressure of $CaSiO_3$ perovskite was examined using multianvil apparatus (Gasparik et al., 1994; Wang and Weidner, 1994) and diamond anvil cell (Shim et al., 2000), the results have shown a large discrepancy in pressure of about 5 GPa. In this study, we have examined the transition of walstromite to larnite + titanite and to $CaSiO_3$ perovskite by high-pressure experiments. Using high-temperature calorimetric techniques, we have also measured enthalpies of the $CaSiO_3$ polymorphs and of titanite solid solutions in the system $CaTiSiO_5$–$CaSi_2O_5$. The former data have been used to obtain the transition enthalpies, and the latter to accurately estimate enthalpy of formation of $CaSi_2O_5$ titanite. The thermodynamic data are used to constrain the transition boundaries in $CaSiO_3$ by combining the above high-pressure experimental data. We also discuss some applications of our results to estimate the depth of formation of $CaSiO_3$ perovskite in the pyrolitic mantle, as well as of high-pressure calcium silicates found in natural diamonds.

2. Experimental methods

2.1. Synthesis of samples

Starting materials of high-pressure transition experiments and samples used for calorimetric measurements were prepared using reagent grade chemicals, as follows.

$CaMgSi_2O_6$ diopside was made from a stoichiometric mixture of $CaCO_3$, MgO, and SiO_2·11 wt.%H_2O silicic acid. The mixture was heated at 1550 °C for 1 h, and quenched to form a glass. The glass was kept at 1250 °C for 3 days to crystallize diopside that was confirmed as single-phase material of $CaMgSi_2O_6$ composition with powder X-ray diffraction and EPMA analysis.

Glasses with nominal compositions of $(Mg_{1-x}, Ca_x)SiO_3$ (x = 0.05, 0.10, 1.00) were made from stoichiometric mixtures of $CaCO_3$, MgO, and SiO_2·11 wt.%H_2O. The mixtures were heated at 1550–1700 °C, and quenched to form glasses. EPMA analysis indicated that the glasses were homogeneous with compositions of $(Mg_{0.947},Ca_{0.053})SiO_3$, $(Mg_{0.891},Ca_{0.109})SiO_3$ and $CaSiO_3$.

From a stoichiometric mixture of $CaCO_3$ and SiO_2·11 wt.%H_2O, $CaSiO_3$ pseudowollastonite was prepared by heating at 1350 °C for 30 h, and $CaSiO_3$ wollastonite at 950 °C for 73 h. Both the samples were confirmed to be single-phase materials by powder X-ray diffraction. $CaSiO_3$ walstromite was synthesised from pseudowollastonite at 5 GPa and 1200 °C for 2 h in a Pt capsule with 12 mm edge anvils using a Kawai-type 6–8 multianvil apparatus described below.

$CaSi_{2-x}Ti_xO_5$ titanite solid solutions (x = 0.10, 0.20, 0.50, 0.75) were made as follows. First, glasses of the above nominal compositions were prepared from stoichiometric mixtures of $CaCO_3$, TiO_2 and SiO_2·11 wt.%H_2O by heating at 1650 °C for 1 h and quenching. EPMA analysis indicated that the glasses had the above compositions within the errors. The glasses were kept at 11 GPa and 1300 °C for 4 h in a Pt capsule using 8 mm edge length anvils. $CaTiSiO_5$ titanite was synthesised at 1 atm. as follows. A stoichiometric mixture of $CaCO_3$, TiO_2 and SiO_2·11 wt.%H_2O was melted at 1200–1400 °C for 34 h and quenched to form $CaTiSiO_5$ glass, and the glass was crystallised at 1050–1100 °C for 124 h. All of the synthesised samples of $CaSi_{2-x}Ti_xO_5$

($x = 0.10, 0.20, 0.50, 0.75, 1.00$) were examined by powder X-ray diffraction, thus confirming them to be single-phase materials with the titanite structure.

2.2. High-pressure experiments

Phase relations in $CaMgSi_2O_6$ and $CaSiO_3$ at high pressures and high temperatures were examined in detail using the Kawai-type multianvil apparatus. The experiments at pressures above and below 14 GPa were made using tungsten carbide anvils with truncated edge lengths of 2.5 and 5 mm, respectively. Semi-sintered MgO·5 wt.% Cr_2O_3 octahedra of 7 and 10 mm edge lengths were used as pressure media with the 2.5 and 5 mm edge length anvils, respectively. In both cells, a cylindrical Re or Pt furnace/capsule of 30 μm wall thickness was used, and a $LaCrO_3$ sleeve was placed outside of the furnace for thermal insulation. A powdered sample was put directly into the furnace with two $LaCrO_3$ plugs at both ends of the heater. Two Pt discs were inserted between the plugs and the sample to avoid reaction. In the $CaMgSi_2O_6$ runs using the 2.5 mm anvils, diopside powder of 0.6 mm thickness was put into the central part of Re furnace of 1.2 mm diameter and 5.7 mm length. In two $CaSiO_3$ runs at 14–15.2 GPa using 2.5 mm anvils, the sample chamber was divided with a thin BN disc into two parts both of which were 0.6 mm in thickness, and wollastonite and α-Mg_2SiO_4 were put in two portions of the chamber. In the $CaSiO_3$ runs using the 5 mm anvils, $CaSiO_3$ glass powder of 1.0 mm thickness was packed in the central part of Pt heater of 2 mm in diameter and 8 mm in length. In all of the runs, temperature was measured on the outer surface in the central part of the heater with a Pt/Pt–13%Rh thermocouple without correction for the pressure effect on emf.

Pressure was calibrated at room temperature using pressure fixed points of Bi I–II (2.55 GPa), Ba I–II (5.5), Bi III–V (7.7), Ba II–III (12.3), ZnS (15.5), GaAs (18.3) and GaP (23). The pressure was further corrected at 1200, 1600 and 1800 °C using α–β and β–γ transition boundaries of Mg_2SiO_4 by Katsura and Ito (1989) which agree well with those determined by in situ X-ray measurements of Morishima et al. (1994) and Suzuki et al. (2000) in the above temperature range. Relative uncertainty of pressure was within about 0.3 GPa. The starting material was kept at 5–23 GPa and 1000–2000 °C for 0.2–10 h, quenched and recovered to ambient conditions. Temperature was controlled generally within ±20 °C. In most of the runs, the run product was polished, and the phases near the thermocouple junction were examined by a microfocus X-ray diffractometer with Cr radiation operated at 40 kV and 250 mA with X-ray beam collimated to 50 μm in diameter. In some runs, the recovered sample was crushed, and lattice parameters were measured by a powder X-ray diffractometer with Cr radiation. The powder diffraction profiles of tetragonal garnets (Gt) in the system $MgSiO_3$–$CaSiO_3$ were analysed with profile-fit software named Peak Fit (SPSS Inc.).

2.3. Calorimetry

A twin Calvet-type microcalorimeter was used to measure solution enthalpies of the samples. The calorimeter was operated at 705 °C, and lead borate ($2PbO·B_2O_3$) was used as a solvent. Three types of calorimetric experiments were performed to measure enthalpies. The first type was solution calorimetry in which a powder sample of about 5–10 mg was kept in a Pt cup just above the solvent surface in the calorimeter for several hours for thermal equilibration, and then dissolved in the solvent by several stirs. Enthalpies of solution at 705 °C for $CaSiO_3$ wollastonite and walstromite were measured using this method. A more detailed description of this method is given in Akaogi et al. (1990). The second type experiment was differential drop-solution calorimetry that is described in detail by Akaogi et al. (1995). A powder sample of about 3–8 mg and a Pt wire contained in a thin silica glass capsule were dropped from room temperature into the solvent in one side of the calorimeter detector at 705 °C. The sample and the silica glass capsule were completely dissolved in the solvent. Simultaneously, the other silica glass capsule and the Pt wire were dropped into the other side of the calorimeter. The weights of the two capsules and those of the two Pt wires were chosen to cancel the heat effects in the two detectors of the twin calorimeter. This method was applied to measure drop-solution enthalpies for most of the samples. The third type experiment was drop-solution calorimetry using a technique which bubbles Ar gas. This method was developed by Navrotsky et al. (1994). Because Ti-rich samples generally dissolved very slowly in lead borate solvent,

we allowed Ar to flow into the solvent at a rate of 6.5 cm^3/min to produce bubbles in order to enhance dissolution of $CaSi_{2-x}Ti_xO_5$ titanite solid solutions ($x = 0.5, 0.75, 1.0$). The powder sample of titanite solid solution of about 3–6 mg was pressed into a pellet, dropped from room temperature into the solvent, and dissolved completely by the gas-bubbling technique. A more detailed description of this method will be given in a separate paper. In all the three types of experiments, seven to eleven measurements were repeated to obtain data of high precision.

3. Results and discussion

3.1. High-pressure transitions in $CaMgSi_2O_6$

The results of high-pressure experiments on $CaMgSi_2O_6$ are summarised in Table 1, and the phase relations are illustrated in Fig. 1. Observed crystalline phases are diopside, garnet, β-phase (wadsleyite), spinel (ringwoodite), stishovite, ilmenite (akimotoite) and Mg-perovskite. In addition, an amorphous phase with almost $CaSiO_3$ composition was found by EPMA analysis, and was interpreted as a retrogressive transformation product of Ca-perovskite. At 1000–1800 °C, diopside is stable up to about 17–18 GPa, above which it transforms to two different high-pressure phase assemblages, depending on temperature. Below

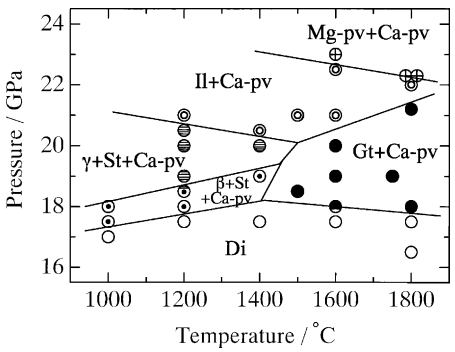

Fig. 1. Phase relations in $CaMgSi_2O_6$. Open and solid circles indicate product phases of diopside (Di) and of garnet (Gt) + Ca-perovskite (Ca-pv), respectively. Circles with a dot and those with lines represent β-phase + stishovite (St) + Ca-perovskite and γ-phase + stishovite + Ca-perovskite, respectively. Double circles and circles with cross indicate ilmenite (Il) + Ca-perovskite and Mg-perovskite (Mg-pv) + Ca-perovskite, respectively.

about 1400 °C, diopside dissociates into an assemblage of β-Mg_2SiO_4, stishovite and Ca-perovskite at 17–18 GPa, and further to γ-Mg_2SiO_4, stishovite and Ca-perovskite at 18–19 GPa. The observed transition pressure between the two assemblages is generally consistent with the β–γ transition of Mg_2SiO_4 reported by Katsura and Ito (1989) and Suzuki et al. (2000). The mixture of γ-Mg_2SiO_4, stishovite, and Ca-perovskite changes into an assemblage of ilmenite and Ca-perovskite at about 21 GPa. At temperatures above about 1400 °C, diopside dissociates into a mixture of garnet and Ca-perovskite. This assemblage changes to ilmenite + Ca-perovskite at 20–21 GPa, and the ilmenite further transforms to Mg-perovskite at 22–23 GPa, as shown in Fig. 1. The dissociation boundary of diopside to garnet + Ca-perovskite has a small negative slope, in contrast to the positive slope boundary for dissociation of diopside to the mixture of β-Mg_2SiO_4, stishovite and Ca-perovskite. The stability of garnet + Ca-perovskite at relatively high-temperature is consistent with the results by Canil (1994), Gasparik (1996), and Oguri et al. (1997). However, Canil's (1994) result that diopside dissociated directly into $MgSiO_3$ ilmenite+Ca-perovskite at 18–19 GPa below 1300 °C contradicts our results that show decomposition to β-Mg_2SiO_4 + stishovite + Ca-perovskite. Although the reason for the difference is not clear, ilmenite in the dissociation product in Canil's experiments might be a metastable phase, because phase transition experiments in $MgSiO_3$ by Ito and Navrotsky (1985) indicate that β- or γ-Mg_2SiO_4 + stishovite is stable at 17–19 GPa at 1300 °C, instead of $MgSiO_3$ ilmenite. As shown in Fig. 1, the stability field of the assemblage of β-Mg_2SiO_4, stishovite and Ca-perovskite is very narrow within only about 1 GPa. This would be the reason why Koito et al. (2000) did not observe the narrow field in their study in which the experiments were made with 1 GPa intervals.

Table 2 shows the results of EPMA analysis of coexisting garnet and Ca-perovskite in two different run products. At 19 GPa and 1750 °C, garnet contains about 16 mol% $CaSiO_3$ component in the system $MgSiO_3$–$CaSiO_3$, while Ca-perovskite contains only about 3 mol% $MgSiO_3$ component. However, garnet containing 27 mol% $MgSiO_3$ coexists with Ca-perovskite having 8 mol% $MgSiO_3$ at 19.4 GPa and about 2000 °C. This indicates that mutual solubilities of $MgSiO_3$ and $CaSiO_3$ components in garnet

Table 1
Experimental results on high-pressure transitions in $CaMgSi_2O_6$

Run no.	Pressure (GPa)	Temperature (°C)	Duration (h)	Phases present
D34	17.0	1000	5	cpx
D33	17.5	1000	5	β + st + Ca-pv
D28	18.0	1000	5	β + st + Ca-pv
D25	17.5	1200	3	cpx
D23	18.0	1200	3	β + st + Ca-pv
D27	18.5	1200	3	β + γ + st + Ca-pv
D11	19.0	1200	3	γ + st + Ca-pv
D16	20.0	1200	3	γ + st + Ca-pv
D15	20.5	1200	3	γ + st + Ca-pv
D18	21.0	1200	3	il + Ca-pv
D38	17.5	1400	2	cpx
D20	19.0	1400	2	β + st + Ca-pv
D19	20.0	1400	2	γ + st + Ca-pv
D17	20.5	1400	2	il + Ca-pv
D12	18.5	1500	2	gt + Ca-pv
D22	21.0	1500	2	il + Ca-pv
D26	17.5	1600	1	cpx
D30	18.0	1600	1	gt + Ca-pv
D21A	19.0	1600	3	gt + Ca-pv
D29	20.0	1600	1.5	gt + Ca-pv
D24[a]	21.0	1600	1	il + Ca-pv
D35	22.5	1600	1	il + Ca-pv
D1A	23.0	1600	1	Mg-pv + Ca-pv
D21	19.0	1750	3	gt + Ca-pv
D36	16.5	1800	1	cpx
D37	17.5	1800	1	cpx
D39	18.0	1800	1	gt + Ca-pv
D31	21.2	1800	1	gt + Ca-pv
D41	22.0	1800	1	il + Ca-pv
D32	22.3	1800	1	Mg-pv + Ca-pv
D40	22.3	1800	1	Mg-pv + Ca-pv
M16[a]	19.4	2000	0.2	gt + Ca-pv
G5[b]	19.0	1600	1	gt
G10[c]	19.0	1600	1	gt

cpx: clinopyroxene, gt: garnet, st: stishovite, β: β-Mg_2SiO_4, γ: γ-Mg_2SiO_4, il: ilmenite, Mg-pv: Mg-perovskite, Ca-pv: Ca-perovskite.
[a] Temperature was estimated by temperature–power relationship because of thermocouple failure.
[b] Starting material was $(Mg_{0.947},Ca_{0.053})SiO_3$ glass.
[c] Starting material was $(Mg_{0.891},Ca_{0.109})SiO_3$ glass. In all other runs, $CaMgSi_2O_6$ diopside was used as the starting material.

and Ca-perovskite increase with increasing temperature. X-ray powder diffraction patterns show that garnet coexisting with Ca-perovskite has a tetragonal symmetry similar to $MgSiO_3$ garnet. Table 3 shows the lattice parameters and cell volume of garnet in the run product of diopside at 19 GPa and 1600 °C, together with those of single-phase garnets synthesised from $(Mg_{1-x},Ca_x)SiO_3$ glasses ($x = 0.053$, 0.109). Fig. 2 shows the relationship of the cell parameters and volume with $CaSiO_3$ content. The figure includes our data together with previous data on precisely determined cell parameters of $MgSiO_3$ garnet (Matsubara et al., 1990; Yagi et al., 1992) and $(Mg_{0.878},Ca_{0.122})SiO_3$ garnet (Hazen et al., 1994). All the data plot almost on straight lines, as shown in Fig. 2. Using this linear relationship, the garnet in the diopside run at 19 GPa and 1600 °C is estimated to contain about 10 mol% $CaSiO_3$. Thus, combination of this value with those in Table 2 confirms that the $CaSiO_3$ component in garnet coexisting with Ca-perovskite increases with temperature. It is also interesting to compare the two-phase stability field of

Table 2
Results of EPMA analysis of phases in the runs of $CaMgSi_2O_6$

wt.%	Run no.			
	D21		M16	
	Gt	Ca-pv	Gt	Ca-pv
SiO_2	57.54	50.62	56.51	50.22
MgO	32.37	0.84	26.83	2.51
CaO	8.68	44.60	13.52	42.06
Total	98.59	96.06	96.86	94.79
Si	1.000	1.010	1.012	1.010
Mg	0.838	0.025	0.716	0.075
Ca	0.162	0.954	0.260	0.906
Total	2.000	1.989	1.988	1.991
Ca/(Mg + Ca)	0.162	0.974	0.266	0.924

Numbers of cation are on the basis of three-oxygen formula.

Table 3
Lattice parameters and volumes of garnets in the system $MgSiO_3$–$CaSiO_3$

Composition	a(Å)	c(Å)	V(Å^3)
$(Mg_{0.947},Ca_{0.053})SiO_3$[a]	11.537(2)	11.460(4)	1525.4(6)
$(Mg_{0.891},Ca_{0.109})SiO_3$[a]	11.581(2)	11.517(4)	1544.5(6)
$(Mg_{1-x},Ca_x)SiO_3$[b]	11.573(2)	11.502(3)	1540.5(5)

[a] Garnet synthesized from glass of the composition shown above.

[b] Garnet synthesised from diopside at 19 GPa and 1600 °C (run no. D21A).

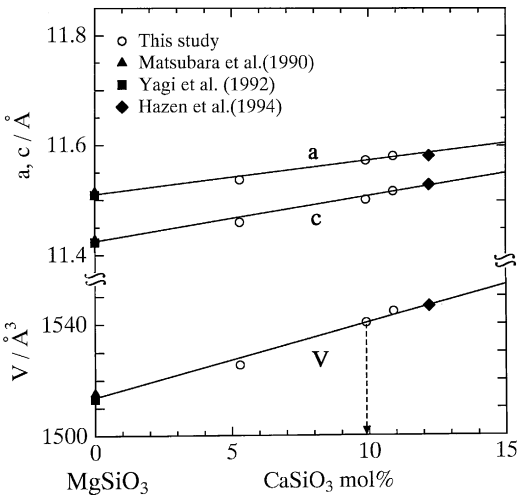

Fig. 2. Lattice parameters and cell volumes of tetragonal garnets in the system $MgSiO_3$–$CaSiO_3$. An arrow indicates the estimated composition of garnet in the diopside run (run no. D21A), using the cell volume–composition relationship.

Table 4
Experimental results on high-pressure transitions in $CaSiO_3$

Run no.	Pressure (GPa)	Temperature (°C)	Duration (h)	Phases present
W1	9.5	1000	3	wal
W10	9.8	1000	1.3	tri + tit + lar
W11	5.0	1200	2	wal
W4	9.6	1200	1	wal
W5	10.2	1200	1.3	tri + lar
W6	10.6	1200	10	tri + lar
W7	9.8	1400	1.4	wal
W8	10.1	1400	1.1	tri + tit + lar
W9	10.4	1400	1	tri + tit + lar
WF2[a]	14.0	1600	3	tit + tri + lar/ α-Mg_2SiO_4
WF1[a]	15.2	1600	3	Ca-pv/β-Mg_2SiO_4

[a] Two starting materials, $CaSiO_3$ wollastonite and α-Mg_2SiO_4, were put into separate portions of the sample chamber. wal: $CaSiO_3$ walstromite; tit: $CaSi_2O_5$ titanite; tri: $CaSi_2O_5$ triclinic phase; Ca-pv: Ca-perovskite.

(Mg,Ca)SiO_3 garnet and Ca-perovskite in Fig. 1 with the field of pure $MgSiO_3$ garnet (Yusa et al., 1993). The field of garnet + Ca-perovskite in diopside expands to lower temperature and to higher pressure, compared with that of $MgSiO_3$ garnet. This indicates that dissolution of the $CaSiO_3$ component expands the garnet field to a wider P–T space, as suggested by Oguri et al. (1997).

3.2. High-pressure transitions in $CaSiO_3$

The results of $CaSiO_3$ transition experiments at 5–16 GPa are shown in Table 4, and the phase relations are illustrated in Fig. 3a together with the data by Gasparik et al. (1994). The data on the wollastonite–walstromite transition by Essene (1974) and Huang and Wyllie (1975) are also included in Fig. 3a. Our data indicate that $CaSiO_3$ walstromite is stable at pressures up to 9–10 GPa above which it dissociates to a mixture of Ca_2SiO_4 and $CaSi_2O_5$, and that the dissociation boundary has a positive slope. Powder X-ray diffraction patterns of the recovered samples indicate that Ca_2SiO_4 larnite coexists with titanite and/or triclinic phase of $CaSi_2O_5$. This is consistent with previous studies: Wang and Weidner (1994) confirmed by in situ X-ray measurements that the dissociation phases were Ca_2SiO_4 larnite and $CaSi_2O_5$ titanite at high-pressure and

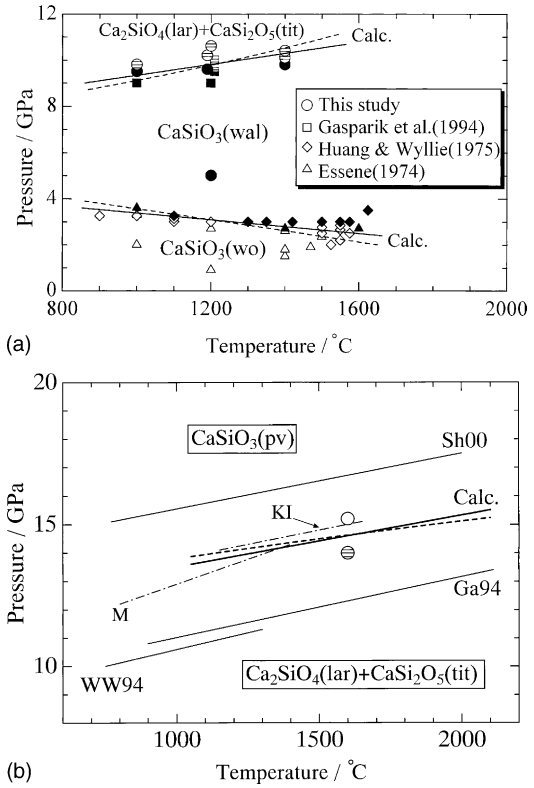

Fig. 3. Phase relations in $CaSiO_3$. (a) The wollastonite (wo)-walstromite (wal) transition and the dissociation of walstromite to larnite (lar) + titanite (tit). Solid lines indicate calculated transition boundaries without corrections for effects of pressure and temperature on thermodynamic parameters, and dashed lines with the corrections (see text). (b) The transition between larnite + titanite and Ca-perovskite. An open circle and a lined circle show the products of Ca-perovskite and of larnite + titanite, respectively (see text). A thick solid line represents the transition boundary without the above corrections, and a thick dashed line the boundary with the corrections. WW94, Ga94 and Sh00 represent the boundaries reported by Wang and Weidner (1994), Gasparik et al. (1994) and Shim et al. (2000), respectively. KI and M show the α–β transition boundaries of Mg_2SiO_4 by Katsura and Ito (1989) and Morishima et al. (1994), respectively.

high-temperature, and Angel et al. (1996) reported that the titanite transformed to a triclinic phase upon decompression.

The boundary for the transition of larnite + titanite to $CaSiO_3$ perovskite has been determined, using multianvil apparatus (Gasparik et al., 1994; Wang and Weidner, 1994) and diamond anvil cell (Shim et al., 2000), and the results are shown in Fig. 3b. The boundary by Wang and Weidner (1994) is regarded as a lower bound, because they observed the appearance of larnite and titanite from single-phase Ca-perovskite in decompression experiments at high-temperature by in situ X-ray measurements. Gasparik et al.'s (1994) boundary based on quench experiments is located at a very similar position to that of Wang and Weidner (1994). On the other hand, Shim et al. (2000) suggested that their boundary had an uncertainty of ±2 GPa and could be regarded as an upper bound, because they observed in situ the phases during pressure increase. Fig. 3b indicates the large discrepancy among the boundaries reported in these studies. Because these results suggest that the real equilibrium boundary would be placed between Shim et al. (2000) and Wang and Weidner (1994), we intended to determine the boundary for $CaSiO_3$ perovskite formation more accurately, using the α–β transition in Mg_2SiO_4 for pressure calibration which would be expected to be very close to that of the perovskite formation boundary. We examined the transitions of $CaSiO_3$ and Mg_2SiO_4 at the same P, T conditions in the single run by quench experiments. Our results are shown in Fig. 3b which includes the α–β transition boundaries of Mg_2SiO_4 determined by Morishima et al.'s (1994) in situ X-ray measurements and by Katsura and Ito's (1989) quench experiments. In our run product at 15.2 GPa and 1600 °C, we observed β-Mg_2SiO_4 and an amorphous phase derived from Ca-perovskite. But a mixture of larnite, titanite and triclinic phase was observed together with α-Mg_2SiO_4 in the run product at 14 GPa and 1600 °C. Both of the results indicate that at 1600 °C the transition pressure of larnite + titanite to Ca-perovskite is 14.6 ± 0.6 GPa and is very close to that of the α–β transition in Mg_2SiO_4. Therefore, Fig. 3b indicates that the Ca-perovskite formation pressure has been more tightly constrained than in the previous studies.

3.3. *Calorimetry of $CaSiO_3$ phases and $CaSi_2O_5$–$CaTiSiO_5$ titanites*

Measured enthalpies of $CaSiO_3$ polymorphs and titanites in the system $CaSi_2O_5$–$CaTiSiO_5$ are summarised in Table 5. Our solution enthalpies of wollastonite and walstromite in Table 5 are in good agreement with Charlu et al.'s (1978) data, 29.6 ± 0.9 and 22.7 ± 0.6 kJ/mol, respectively, mea-

Table 5
Measured drop-solution enthalpies and solution enthalpies of phases in the system $CaO–SiO_2–TiO_2$

Phase	$\Delta H^\circ_{d\text{-}s}$ (kJ/mol)	$\Delta H^\circ_{s,978}$ (kJ/mol)
$CaSiO_3$ wollastonite	103.47 ± 3.99 [11]	29.55 ± 2.22 [7]
$CaSiO_3$ walstromite	93.07 ± 2.16 [10]	20.44 ± 1.81 [7]
$CaTi_{0.1}Si_{1.9}O_5$ titanite	93.45 ± 2.41 [10]	–
$CaTi_{0.2}Si_{1.8}O_5$ titanite	109.79 ± 5.40 [11]	–
$CaTi_{0.5}Si_{1.5}O_5$ titanite	134.91 ± 3.20 [11]	–
$CaTi_{0.75}Si_{1.25}O_5$ titanite	166.07 ± 2.47 [9]	–
$CaTiSiO_5$ titanite	191.95 ± 3.70 [9]	–
CaO rock salt	−23.10 ± 1.66 [8]	–
SiO_2 quartz[a]	40.05 ± 0.36 [6]	−3.56 ± 0.22 [8]

[a] Akaogi et al. (1995). $\Delta H^\circ_{d\text{-}s}$: drop-solution enthalpy, $\Delta H^\circ_{s,978}$: solution enthalpy at 978 K. Number in brackets represents number of experimental runs.

sured in $2PbO{\cdot}B_2O_3$ solvent at 697 °C. The measured drop-solution enthalpy ($\Delta H^\circ_{d\text{-}s}$) of $CaSiO_3$ wollastonite is consistent with 104.6 ± 0.5 kJ/mol measured by Kojitani et al. (2001). The drop-solution enthalpy of SiO_2 quartz was measured by Akaogi et al. (1995) by using the same calorimetric technique. Using the measured enthalpies in Table 5, we calculate enthalpies of formation at 298 K ($\Delta H^\circ_{f,298}$) of wollastonite and walstromite from CaO + SiO_2 (quartz), e.g. as follows,

$$\Delta H^\circ_{f,298}(\mathrm{wo}) = \Delta H^\circ_{d\text{-}s}(\mathrm{CaO}) + \Delta H^\circ_{d\text{-}s}(\mathrm{qz}) - \Delta H^\circ_{d\text{-}s}(\mathrm{wo}) \quad (1)$$

The obtained $\Delta H^\circ_{f,298}$ values are shown in Table 6. Our $\Delta H^\circ_{f,298}$ data for wollastonite and walstromite are consistent with −89.0 kJ/mol for wollastonite by Robie and Hemingway (1995) and −78.9 ± 1.4 kJ/mol for walstromite by Kojitani et al. (2001), respectively. Based on drop-solution enthalpy data for perovskite solid solutions in the system $CaSiO_3–CaGeO_3$, Kojitani et al. (2001) estimated $\Delta H^\circ_{f,298}$ of $CaSiO_3$ perovskite, as shown in Table 6. This value agrees well with that obtained from the data on perovskites in the system $CaSiO_3–CaTiO_3$ by Koito et al. (2000).

Table 6
Molar volumes and enthalpies of formation of calcium silicates from CaO and SiO_2 quartz at 298 K

Phase	$\Delta H^\circ_{f,278}$ (kJ/mol)	V°_{298} (cm^3/mol)
$CaSiO_3$ wollastonite	−86.52 ± 4.34[a]	39.93[b]
$CaSiO_3$ walstromite	−76.12 ± 2.75[a]	37.94[b]
$CaSi_2O_5$ titanite	−27.82 ± 2.12[a]	48.25[c]
Ca_2SiO_4 larnite	−125.80 ± 2.55[d]	51.79[e]
$CaSiO_3$ perovskite	14.79 ± 4.41[f]	27.45[g]

[a] This study.
[b] Chatterjee et al. (1984).
[c] Kanzaki et al. (1991).
[d] Robie and Hemingway (1995).
[e] Jost et al. (1977).
[f] Kojitani et al. (2001).
[g] Wang et al. (1996).

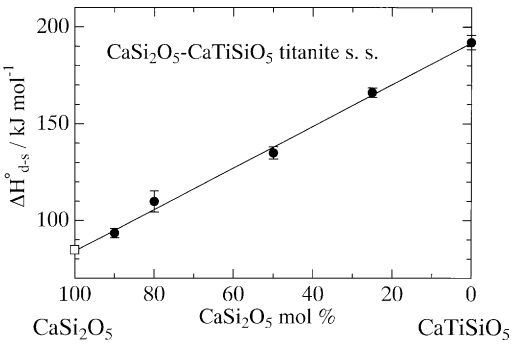

Fig. 4. Drop-solution enthalpies of titanite solid solutions in the system $CaSi_2O_5–CaTiSiO_5$. Solid circles show the measured data, and an open square the estimated enthalpy for $CaSi_2O_5$ titanite.

To estimate the enthalpy of formation of $CaSi_2O_5$ titanite, we measured drop-solution enthalpies of titanite solid solutions in the system $CaSi_2O_5–CaTiSiO_5$, and the results are shown in Table 5 and Fig. 4. The $\Delta H^\circ_{d\text{-}s}$ of $CaTiSiO_5$ titanite in Table 5 is consistent with 195.6 ± 2.4 kJ/mol by Xirouchakis et al. (1997). The drop-solution enthalpies of the five titanite solid solutions are plotted in Fig. 4 and lie on a straight line within the errors, indicating that mixing enthalpy of titanite in the system $CaSi_2O_5–CaTiSiO_5$ is negligibly small. This is compatible with no excess volume of mixing in titanite solid solution in the system reported by Knoche et al. (1998). Therefore, by assuming zero mixing enthalpy for titanite solid solution, we extrapolate linearly the measured enthalpies to $CaSi_2O_5$ composition to obtain 84.8 ± 1.1 kJ/mol for $CaSi_2O_5$ titanite. Thus, enthalpy of formation of $CaSi_2O_5$ titanite for CaO and SiO_2 quartz at 298 K is calculated as −27.8 ± 2.1 kJ/mol. Schoenitz et al. (2001) obtained the $\Delta H^\circ_{f,298}$ of $CaSi_2O_5$ triclinic phase to be −26.3 ± 4.3 kJ/mol, based on drop-solution calorimetry. Therefore, the enthalpy difference between the two polymorphs is a very small value, 1.5 ± 4.8 kJ/mol. Swamy and Dubrovinsky (1997) de-

rived an internally consistent thermodynamic data set for the high-pressure phases in the system CaO–SiO_2. Their estimated enthalpy of formation of $CaSi_2O_5$ titanite from CaO + SiO_2 at 298 K is −30.4 kJ/mol. This value is marginally consistent with our datum for $CaSi_2O_5$ titanite, though Swamy and Dubrovinsky's value depends on input data which are not well constrained. Warren et al. (1999) reported that the triclinic phase would be about 14 kJ/mol more stable than titanite at 0 K on the basis of first principle calculations. However, our enthalpy difference is smaller than their calculation.

3.4. Calculation of high-pressure phase relations in $CaSiO_3$

Using the $\Delta H^{\circ}_{f,298}$ values in Table 6, enthalpies of transitions in $CaSiO_3$ at 298 K are calculated for the following reactions

$$CaSiO_3(wo) = CaSiO_3(wal) \quad (2)$$

$$CaSiO_3(wal) = \tfrac{1}{3}Ca_2SiO_4(lar) + \tfrac{1}{3}CaSi_2O_5(tit) \quad (3)$$

$$\tfrac{1}{3}Ca_2SiO_4(lar) + \tfrac{1}{3}CaSi_2O_5(tit) = CaSiO_3(pv) \quad (4)$$

as 10.4 ± 4.5, 24.9 ± 3.0 and 66.0 ± 4.5 kJ/mol, respectively. The $\Delta H^{\circ}_{f,298}$ for reaction (2) is slightly larger than the enthalpy of transition at 978 K, 9.1 ± 2.9 kJ/mol, calculated from $\Delta H^{\circ}_{f,298}$ in Table 5. We calculate equilibrium transition boundaries of $CaSiO_3$ using the above transition enthalpies at 298 K and molar volumes shown in Table 6. Although the phase transition of larnite to α'_L (or α'_H)-Ca_2SiO_4 was suggested by in situ X-ray studies at around 9 GPa at relatively high-temperature (Wang and Weidner, 1994; Shim et al., 2000), we do not include the transition boundary involving α'_L (or α'_H)-Ca_2SiO_4. This is because the α'_L- and α'_H-phases have structures very similar to larnite and, therefore, are expected to have similar thermodynamic properties to larnite. In addition, the larnite-α'_L (or α'_H) transition boundary has not yet been experimentally constrained in the 8–12 GPa range. A transition boundary is calculated by the equation,

$$\Delta G_{P,T} = \Delta H^{\circ} - T\Delta S^{\circ} + \int_1^P \Delta V_{P,T}\,dP = 0 \quad (5)$$

where ΔH° and ΔS° are the enthalpy and entropy of transition, respectively, at T and 1 atm., and $\Delta G_{P,T}$ and $\Delta V_{P,T}$ are free energy change and volume difference, respectively, at P and T. The entropy of transition is determined from ΔH° and $\Delta V_{P,T}$ by choosing one P,T point assumed to be on the equilibrium transition boundary. Firstly, we do not correct effects of temperature on ΔH° and ΔS° and those of pressure and temperature on $\Delta V_{P,T}$, because the effects would be generally small, and furthermore heat capacities, thermal expansivities, and bulk moduli of $CaSiO_3$ walstromite, Ca_2SiO_4 larnite and $CaSi_2O_5$ titanite and the heat capacity of $CaSiO_3$ perovskite have not yet been measured or are poorly constrained. For the wollastonite–walstromite transition, we select 3.1 GPa at 1200 °C as the fixed point, and the calculated boundary is shown in Fig. 3a. The calculated ΔS° and boundary slope are 2.9 ± 3.1 J/mol K and −1.5 ± 1.6 MPa/K, respectively. As shown in Fig. 3a, the calculated boundary is consistent with the experimental data determined using piston-cylinder apparatus by Essene (1974) and Huang and Wyllie (1975). The dissociation boundary of $CaSiO_3$ walstromite to Ca_2SiO_4 larnite + $CaSi_2O_5$ titanite is calculated using the above transition enthalpy by adopting 9.8 GPa at 1200 °C as the fixed point. The calculated ΔS° and the boundary slope are −13.7 ± 2.0 J/mol K and 3.0 ± 0.4 MPa/K, respectively. When the uncertainty of the slope is considered, the calculated boundary agrees well with our experimental runs shown in Fig. 3a. To calculate the boundary from Ca_2SiO_4 larnite + $CaSi_2O_5$ titanite to $CaSiO_3$ perovskite, we adopt 14.6 GPa at 1600 °C as the fixed point on the basis of our runs shown in Table 4 and Fig. 3b. The calculated ΔS° is −10.7 ± 2.4 J/mol K, and the calculated boundary shown in Fig. 3b has a slope of 1.8 ± 0.4 MPa/K. But, when we use 12.4 GPa and 1600 °C, a point on Gasparik et al.'s (1994) boundary, the calculated slope is much smaller, 0.6 ± 0.4 MPa/K which is inconsistent with their boundary. Our experimental runs and thermodynamic calculations constrain the boundary for Ca-perovskite formation more tightly than the previous studies.

Next, we calculate the transition boundaries in $CaSiO_3$ including temperature effects on ΔH° and ΔS° and pressure and temperature effects on $\Delta V_{P,T}$, by adopting tentatively the heat capacities, thermal expansivities, and bulk moduli of the phases in the system CaO–SiO_2 listed by Swamy and Dubrovinsky (1997). The calculation method is the same as that

by Akaogi et al. (1995). By adopting the same fixed points as described above, the transition boundaries are calculated, as shown in Fig. 3a and b. The calculated entropies for the transitions (2), (3) and (4) are 2.7 ± 3.1, -7.9 ± 2.0 and -7.4 ± 2.4 J/mol K, respectively. The calculated slopes of the boundaries for the transitions (2), (3) and (4) are -2.4 ± 1.6, 3.5 ± 0.4 and 1.3 ± 0.4 MPa/K, respectively. Considering the uncertainties, these boundary slopes agree well with those without the corrections. Although some of the heat capacities, thermal expansivities, and bulk moduli used in the calculation are poorly constrained, the calculation suggests that effects of the corrections on the boundary slopes are small.

3.5. Geophysical and petrological implications

Fig. 3b shows that $CaSiO_3$ perovskite becomes stable at about 14 GPa at 1400 °C, conditions that correspond to the pressure and temperature at the top of transition zone (Akaogi et al., 1989). In reality, however, $CaSiO_3$ perovskite would exist in the deeper part of the mantle, because Ca is incorporated in garnet at the top of transition zone. Phase equilibrium experiments in pyrolitic compositions indicate that diopside-rich clinopyroxene is dissolved into pyrope-rich garnet to form majorite garnet solid solution (Gt s.s.), and $CaSiO_3$ perovskite (Ca-pv) is exsolved from the garnet s.s. with increasing depth in the transition zone (Akaogi and Akimoto, 1979; Irifune and Ringwood, 1987; Wood, 2000). This sequence of transitions is expressed as Cpx + Gt → Gt s.s. → Ca-pv + Gt s.s. The depth range of a single Gt s.s. depends on the abundances of Al and Ca in the mantle. In Al-poor and/or Ca-rich compositions, Cpx + Gt changes directly to Ca-pv + Gt s.s. This phase change is expected to occur at a pressure very close to that of the pure $CaMgSi_2O_6$ diopside stability field shown in Fig. 1, because Cpx in the mantle has a diopside-rich composition. This consideration suggests that the dissociation pressure of diopside to $CaSiO_3$ perovskite + $(Mg,Ca)SiO_3$ garnet in Fig. 1 represents the lower limit of stability of $CaSiO_3$ perovskite in the mantle, and that the pressure (or depth) is about 18 GPa (or 520 km) on a normal mantle geotherm. This result is consistent with the idea that the formation of $CaSiO_3$ perovskite from majorite garnet s.s. contributes in part to the so-called "520 km discontinuity", because a significant velocity jump as large as that of β–γ transition in $(Mg,Fe)_2SiO_4$ is associated with the formation of $CaSiO_3$ perovskite (Weidner and Wang, 2000). The recent seismological study by Deuss and Woodhouse (2001) demonstrates that the 520 km discontinuity is split into two discontinuities at about 500 and 560 km depth in a number of areas, but a single 520 km discontinuity is also observed in other areas. This observation suggests that both the wadsleyite-ringwoodite transition and the formation of $CaSiO_3$ perovskite are responsible for the 520 km discontinuity and that the composition and temperature may be rather heterogeneous in the transition zone, resulting in the formation of either a split or a single discontinuity.

Recently, Joswig et al. (1999) reported the natural occurrence of calcium silicate inclusions ($CaSi_2O_5$ titanite, Ca_2SiO_4 larnite and $CaSiO_3$ walstromite) in diamonds from the Kankan district in Guinea. They showed that $CaSi_2O_5$ titanite was found in contact with Ca_2SiO_4 larnite in the same diamond grains and $CaSiO_3$ walstromite in other separate diamonds. On the basis of the phase relations of $CaSiO_3$ shown in Fig. 3, it is suggested that the assemblage of titanite + larnite was equilibrated at about 10–14 GPa (300–420 km depth) and the walstromite at about 4–10 GPa (130–300 km), assuming a normal mantle geotherm.

Acknowledgements

We are very grateful to A. Navrotsky for valuable suggestions on drop-solution calorimetry using the bubbling technique, and to T. Suzuki and K. Yokoyama for their help with EPMA analyses. We also thank A. Woodland for his useful suggestion. Constructive comments by A. Navrotsky and an anonymous referee helped to improve the manuscript. This work was partially supported with Grants-in-aid from Ministry of Education, Science and Culture of Japan and Japan Society for the Promotion of Science.

References

Akaogi, M., Akimoto, S., 1979. High-pressure phase equilibria in a garnet lherzolite, with special reference to Mg^{2+}–Fe^{2+}

partitioning among constituent minerals. Phys. Earth Planet Int. 19, 31–51.

Akaogi, M., Ito, E., Navrotsky, A., 1989. Olivine-modified spinel-spinel transitions in the system Mg_2SiO_4–Fe_2SiO_4: calorimetric measurements, thermochemical calculation, and geophysical application. J. Geophys. Res. 94, 15671–15685.

Akaogi, M., Yusa, H., Ito, E., Yagi, T., Suito, K., Iiyama, J.T., 1990. The $ZnSiO_3$ clinopyroxene-ilmenite transition: heat capacity, enthalpy of transiton, and phase equilibria. Phys. Chem. Miner. 17, 17–23.

Akaogi, M., Yusa, H., Shiraishi, K., Suzuki, T., 1995. Thermodynamic properties of α-quartz, coesite, and stishovite and equilibrium phase relations at high pressures and high temperatures. J. Geophys. Res. 100, 22337–22347.

Angel, R.J., 1997. Transformation of five-coordinated silicon to octahedral silicon in calcium silicate, $CaSi_2O_5$. Am. Miner. 82, 836–839.

Angel, R.J., Ross, N.L., Seifert, F., Fliervoet, T.F., 1996. Structural characterization of penta coordinate silicon in a calcium silicate. Nature 384, 441–444.

Canil, D., 1994. Stability of clinopyroxene at pressure-temperature conditions of the transition zone. Phys. Earth Planet Int. 86, 25–34.

Charlu, T.V., Newton, R.C., Kleppa, O.J., 1978. Enthalpy of formation of some lime silicates by high-temperature solution calorimetry, with discussion of high-pressure phase equilibria. Geochim. Cosmochim. Acta 42, 367–375.

Chatterjee, N.D., Johannes, W., Leistner, H., 1984. The system CaO–Al_2O_3–SiO_2–H_2O: new phase equilibria data, some calculated phase relations, and their petrological applications. Contrib. Mineral. Petrol. 88, 1–13.

Deuss, A., Woodhouse, J., 2001. Seismic observations of splitting of the mid-transition zone discontinuity in Earth's mantle. Science 294, 354–357.

Essene, E., 1974. High-pressure transformations in $CaSiO_3$. Contrib. Mineral. Petrol. 45, 247–250.

Gasparik, T., 1996. Melting experiments on the enstatite-diopside join at 70–224 kbar, including the melting of diopside. Contrib. Mineral. Petrol. 124, 139–153.

Gasparik, T., Wolf, K., Smith, C.M., 1994. Experimental determination of phase relations in the $CaSiO_3$ system from 8 to 15 GPa. Am. Mineral. 79, 1219–1222.

Hazen, R.M., Downs, R.T., Finger, L.W., Conrad, P.G., Gasparik, T., 1994. Crystal chemistry of Ca-bearing majorite. Am. Mineral. 79, 581–584.

Huang, W.-L., Wyllie, P.J., 1975. Melting and subsolidus phase relationships for $CaSiO_3$ to 35 kilobars pressure. Am. Mineral. 60, 213–217.

Irifune, T., Ringwood, 1987. Phase transformations in primitive MORB and pyrolite compositions to 25 GPa and some geophysical implications. In: Manghnani, M.H., Syono, Y. (Eds.), High-Pressure Research in Mineral Physics. Am. Geophys. Union, pp. 221–242.

Ito, E., Navrotsky, A., 1985. $MgSiO_3$ ilmenite: calorimetry, phase equilibria, and decomposition at atmospheric pressure. Am. Mineral. 70, 1020–1026.

Joswig, W., Stachel, T., Harris, J.W., Bauer, W.H., Brey, G.P., 1999. New Ca-silicate inclusions in diamonds: tracers from the lower mantle. Earth Planet Sci. Lett. 173, 1–6.

Jost, K.H., Ziemer, B., Seydel, R., 1977. Redetermination of the structure of β-dicalcium silicate. Acta Cryst. B33, 1696–1700.

Kanzaki, M., Stebbins, J.F., Xue, X., 1991. Characterization of quenched high-pressure phases in $CaSiO_3$ system by XRD and ^{29}Si NMR. Geophys. Res. Lett. 18, 463–466.

Katsura, T., Ito, E., 1989. The system Mg_2SiO_4–Fe_2SiO_4 at high pressures and temperatures: Precise determination of stabilities of olivine, modified spinel, and spinel. J. Geophys. Res. 94, 15663–15670.

Knoche, R., Angel, R.J., Seifert, F., Fliervoet, T.F., 1998. Complete substitution of Si for Ti in titanite $Ca(Ti_{1-x}Si_x)^{VI}Si^{IV}O_5$. Am. Mineral. 83, 1168–1175.

Koito, S., Akaogi, M., Kubota, O., Suzuki, T., 2000. Calorimetric measurements of perovskites in the system $CaTiO_3$–$CaSiO_3$ and experimental and calculated phase equilibria for high-pressure dissociation of diopside. Phys. Earth Planet Int. 120, 1–10.

Kojitani, H., Navrotsky, A., Akaogi, M., 2001. Calorimetric study of perovskite solid solutions in the $CaSiO_3$–$CaGeO_3$ system. Phys. Chem. Miner. 28, 413–420.

Matsubara, R., Toraya, H., Tanaka, S., Sawamoto, H., 1990. Precision lattice-parameter determination of (Mg, Fe)SiO_3 tetragonal garnet. Science 247, 697–699.

Morishima, H., Kato, T., Suto, M., Ohtani, E., Urakawa, S., Utsumi, W., Shimomura, O., Kikegawa, T., 1994. The phase boundary between α- and β-Mg_2SiO_4 determined by in situ X-ray observation. Science 265, 1202–1203.

Navrotsky, A., Rapp, R.P., Smelik, E., Burnley, P., Circone, S., Chai, L., Bose, K., Westrich, H.R., 1994. The behavior of H_2O and CO_2 in high-temperature lead borate solution calorimetry of volatile-bearing phases. Am. Mineral. 79, 1099–1109.

Oguri, K., Funamori, N., Sakai, F., Kondo, T., Uchida, T., Yagi, T., 1997. High-pressure and high-temperature phase relations in diopside $CaMgSi_2O_6$. Phys. Earth Planet Int. 104, 363–370.

Robie, R.A., Hemingway, B.S., 1995. Thermodynamic properties of minerals and related substances at 298.15 K and 1 Bar (10^5 Pascals) pressure and at higher temperatures. US Geol. Surv. Bull. 2131, 461.

Schoenitz, M., Navrotsky, A., Ross, N., 2001. Enthalpy of formation of $CaSi_2O_5$, a quenched high-pressure phase with pentacoordinate silicon. Phys. Chem. Miner. 28, 57–60.

Shim, S.-H., Duffy, T.S., Shen, G., 2000. The stability and P-V-T equation of state of $CaSiO_3$ perovskite in the Earth's lower mantle. J. Geophys. Res. 105, 25955–25968.

Suzuki, A., Ohtani, E., Morishima, H., Kubo, T., Kanbe, Y., Kondo, T., Okada, T., Terasaki, H., Kato, T., Kikegawa, T., 2000. In situ determination of the phase boundary between wadsleyite and ringwoodite in Mg_2SiO_4. Geophys. Res. Lett. 27, 803–806.

Swamy, V., Dubrovinsky, L.S., 1997. Thermodynamic data for the phases in the $CaSiO_3$ system. Geochim. Cosmochim. Acta 61, 1181–1191.

Wang, Y., Weidner, D.J., 1994. Thermoelasticity of $CaSiO_3$ perovskite and implications for the lower mantle. Geophys. Res. Lett. 21, 895–898.

Wang, Y., Weidner, D.J., Guyot, F., 1996. Thermal equation of state of $CaSiO_3$ perovskite. J. Geophys. Res. 101, 661–672.

Weidner, D.J., Wang, Y., 2000. Phase transformations: Implications for mantle structure. In: Karato, S., Forte, A.M., Liebermann, R.C., Masters, G., Stixrude, L. (Eds.), Earth's Deep Interior: Mineral Physics and Tomography from Atomic to the Global Scale. Am. Geophys. Union, pp. 215–235.

Warren, M.C., Redfern, S.A.T., Angel, R., 1999. Change from sixfold to fivefold coordination of silicate polyhedra: insight from first-principles calculations of $CaSi_2O_5$. Phys. Rev. B 59, 9149–9154.

Wood, B.J., 2000. Phase transformations and partitioning relations in peridotite under lower mantle conditions. Earth Planet Sci. Lett. 174, 341–354.

Xirouchakis, D., Fritsch, S., Putnam, R.L., Navrotsky, A., Lindsley, D.H., 1997. Thermochemistry and the enthalpy of formation of synthetic end-member ($CaTiSiO_5$) titanite. Am. Mineral. 82, 754–759.

Yagi, T., Uchiyama, Y., Akaogi, M., Ito, E., 1992. Isothermal compression curve of $MgSiO_3$ tetragonal garnet. Phys. Earth Planet Int. 74, 1–7.

Yusa, H., Akaogi, M., Ito, E., 1993. Calorimetric study of $MgSiO_3$ garnet and pyroxene: heat capacities, transition enthalpies, and equilibrium phase relations in $MgSiO_3$ at high pressures and temperatures. J. Geophys. Res. 98, 6453–6460.